

# Two-Steps Analysis of Movement of the Kfar-Hanassi Network

Gilad EVEN-TZUR, Israel

**Key words:** Deformation network, Two-steps analysis, Distance measurement, Dead Sea Rift

## SUMMARY

The small EDM network at Kfar-Hanassi was established across the Dead Sea Rift (DSR) in the northern part of Israel, where displacements of several millimeters per year between the Sinai sub-plate and the Arabian plate are expected. The results of five campaigns carried out between 1990 and 2008 are presented. Four campaigns were measured annually between 1990 and 1993 using a Mekometer ME5000. An additional campaign was carried out in the summer of 2008 using a Leica TC2002. The large time interval between the campaigns contributed dramatically to the ability of the Kfar-Hanassi network to detect movements.

The distance measurements were analyzed by a Two-Step analysis. In the first step the distance measurements were processed sequentially without modeling the variations in the plane position of the network benchmarks. In the second step the variations in the network geometry were modeled by means of a physical model.

In this study a linear model of movements was tested to describe the plane position of the network benchmarks. The results indicate a left-lateral motion along the DSR with a rate of a few tenths of millimeters per year.

# Two-Steps Analysis of Movement of the Kfar-Hanassi Network

Gilad EVEN-TZUR, Israel

## 1. THE TWO-STEP ANALYSIS METHOD

Two types of models are pertinent in deformation analysis, the mathematical model, representing the geodetic measurements, and the deformation model. The mathematical model is often conceived as being absolutely correct, while the measurements are regarded as quantities corrupted by measurement noise. The deformation model should describe the physical reality, but the validity of the physical model and its system noise is frequently limited.

Estimation of the deformation parameters directly from the geodetic measurements may lead to undesirable results. System noise due to inadequacies of the physical model may cause severe distortions of the parameter estimates.

The relationship between a vector of measurements  $\ell$  and a vector of parameters  $x$  can be expressed by a set of observation equations, given as:

$$\ell = Ax + v \quad (1)$$

Matrix  $A$  denotes the design matrix and  $v$  is the measurement noise vector. It may be assumed that matrix  $A$  is column rank deficient due to the need for datum definition. The parameters  $x$  are calculated under the minimum condition  $v^T P v$ , where  $P$  is the weight matrix of the observations.

Since the vector of parameters  $x$  can be expressed as a linear function of a vector of parameters  $s$ , another set of equations may be created:

$$x = Bs + w \quad (2)$$

where  $B$  is usually a full column rank matrix and  $w$  is the noise vector. The parameters  $s$  are calculated under the minimum condition  $w^T P_x w$ , where  $P_x$  is the weight matrix of the observations in the second model.

This approach for solving  $s$  indirectly from the measurements vector  $\ell$  while using a vector of pseudo-measurements  $x$  is referred to as a Two-Step analysis (Papo and Perelmuter, 1993), where in the first step  $x$  is solved using the measurement vector  $\ell$ , and in the second step  $x$  is used as pseudo-measurements for solving the parameter vector  $s$ .

This paper employs the Two-Steps analysis method for monitoring movements and deformation in the Kfar Hanassi network located in the northern part of Israel.

For  $k$  sets of measurements  $\ell_i$ , each vector of parameters  $x_i$  can be estimated independently as:

$$\hat{x}_i = (A_i^T P_i A_i)^{-1} A_i^T P_i \ell_i \quad (3)$$

with the corresponding cofactor matrix  $Q_{\hat{x}_i} = (A_i^T P_i A_i)^{-1}$  and the variance-covariance matrix

$\Sigma_{\hat{x}_i} = \hat{m}_{0i}^2 Q_{\hat{x}_i}$ , where  $\hat{m}_{0i}^2 = \frac{\hat{v}_i^T P_i \hat{v}_i}{r_i}$ , and  $r_i$  is the adjustment redundancy. The estimated

solution vector  $\hat{x}^T = [\hat{x}_1 \quad \hat{x}_2 \quad \dots \quad \hat{x}_k]^T$  resulting from the first step will be used as pseudo-measurements in the second step.

The set of deformation model parameters  $\hat{s}$  is solved by equation (2) (Papo and Perelmuter, 1993):

$$\hat{s} = (B^T P_x B)^{-1} B^T P_x \hat{x} \quad (4)$$

The weight matrix  $P_x$  is produced by using the variance-covariance matrix  $\Sigma_{\hat{x}}$  instead of the cofactor matrix  $Q_{\hat{x}}$  (Even-Tzur, 2003). The cofactor matrix  $Q_{\hat{s}}$  and the variance-covariance matrix  $\Sigma_{\hat{s}}$  are:

$$Q_{\hat{s}} = (B^T P_x B)^{-1}; \quad \Sigma_{\hat{s}} = \hat{m}_0^2 Q_{\hat{s}} \quad (5)$$

While  $\hat{m}_0^2$  is equal to (Even-Tzur, 2003):

$$\hat{m}_0^2 = \frac{\sum_{i=1}^k r_i + \hat{w}^T Q_x^{-1} \hat{w}}{\sum_{i=1}^k r_i + r_{II}} \quad (6)$$

where  $r_{II}$  is the redundancy of the second step adjustment.

## 2. THE KFAR-HANASSI NETWORK AND FIELD CAMPAIGNS

The Kfar-Hanassi network consists of twelve benchmarks, six benchmarks on each side of the Jordan River gorge in the north of Israel (Fig. 1). The network was established across the Dead Sea Rift (DSR) where displacements of several millimeters per year between the Sinai

sub-plate and Arabian plate are expected. The network spreads over  $2.5 \times 4.0$  km and was designed for EDM measurements. The configuration of the network was mainly affected by the topography of the area and by geomorphological considerations (Steinberg, 1994). The marks were built according to high technical specifications to ensure their geotechnical stability. A borehole, approximately 30 cm in diameter, was drilled to a depth of at least 12 m. The pile consists of concrete reinforcement by steel rods. The upper 3 m long of the pile is isolated from the ground by a sleeve of asphalt paper. Instrument support is provided by three micropiles, 1 m deep and 0.2 m in diameter with tube sockets for the tripod, driven into the ground around the center pile (Karcz, 1994). A more detailed description of the network design and construction is given in Van Mierlo et al. (1990), Van Mierlo and Fahlbusch (1991) and Karcz et al. (1992).

The sensitivity of the network in detecting horizontal movements between the six western benchmarks relative to the six eastern benchmarks was tested by Vogel and Van Mierlo (1994). The network appeared to be more sensitive to displacements in the east-west than in the north-south direction, which is contradictory to the expected displacements in the north-south direction along the Jordan River Gorge.

The network was measured annually during the years 1990-1993 using a Kern Mekometer ME5000. The ME5000 is a very precise distance meter with high intrinsic precision. The field work was done by the Survey of Israel, the Geological Survey of Israel and the geodetic Institute of Karlsruhe University, within the framework of a larger research under the auspices of the German-Israel research Fund (GIF). Since there is no line of sight between points 8 and 12, sixty five distances were measured out of sixty six. Most of the distances were measured twice from each edge of the line (Adler and Pelzer, 1994).

During the summer of 2008 the network was measured once again using a Leica TC2002. The field work was done by the research department of the Survey of Israel. In this campaign four distances were not measured due to line of sight problems (6-11, 7-11, 8-12 and 10-12).

Precise optical plummets were used throughout the campaigns to set up the instrument and prisms over the benchmarks. Meteorological conditions were monitored in detail in the line ends during the measurement process.

The measured distances for each campaign were corrected for the actual meteorological conditions and were reduced to horizontal distances at sea level.

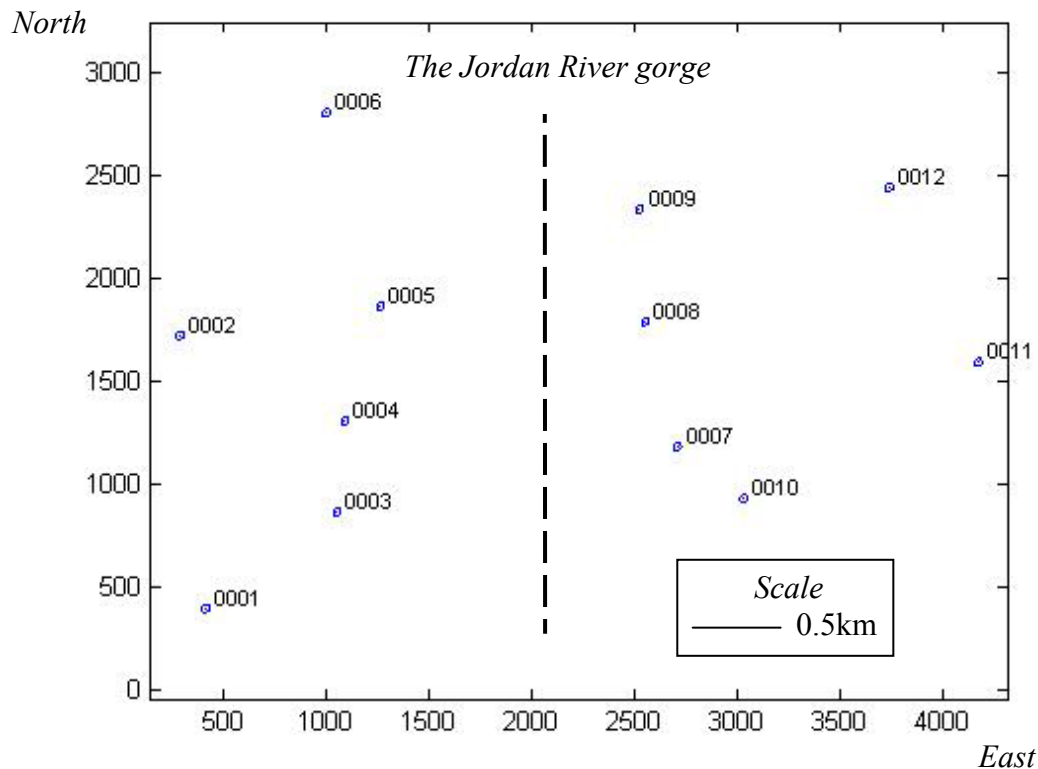


Figure 1 – The Kfar-Hanassi Network

### 3. THE FIRST STEP: EPOCH BY EPOCH DATA PROCESSING

For every measuring campaign the distances were adjusted into a network, while the variance of the observations was modeled by  $\sigma_i^2 = (0.5\text{mm})^2 + (d_i \times 1\text{ppm})^2$  for the ME5000 and  $\sigma_i^2 = (1\text{mm})^2 + (d_i \times 1\text{ppm})^2$  for the TC2002, where  $d_i$  denotes the horizontal distance.

Detection of gross errors was performed using the w-test. Gross errors in the adjusted model will result in the reduction of the quadratic form of the residuals  $(\hat{v}^T P \hat{v})$  by (Chen, 1987 and Etrog, 1991):

$$\Delta R = \hat{v}^T P E (E^T P Q_v P E)^{-1} E^T P \hat{v}, \quad (7)$$

where  $Q_v$  is the Least Squares estimation of the residuals cofactor matrix and E is a matrix with the same number of columns as the number of suspected outliers,  $n_2$ , with a unit value

in the row that correlates to the suspicious observation and zeros in all other rows. The test statistic is  $\Delta R/n_2 m_0^2 \sim F_{\alpha, n_2, \infty}$ , where  $\alpha$  is the significance level and  $m_0^2$  is the a-priori variance factor.

A summary of the network adjustment for each campaign is presented in Table 1. The a-posteriori variance of unit weight,  $\hat{m}_0^2$ , shows that the inner accuracy of the measurements is better than the one that was modeled. The average mean positional error (one sigma) is better than 0.6mm. The network accuracy of the campaigns measured with the ME5000 is slightly better than the one measured with the TC2002.

Monitoring Epoch	Instrument	Distances rejected	Degrees of freedom	Mean positional error (1 sigma)	$\hat{m}_0$
1990.417	ME5000	1-3, 2-6, 3-10	41	0.58mm	0.74
1991.417	ME5000	-	44	0.46mm	0.64
1992.417	ME5000	-	44	0.47mm	0.64
1993.500	ME5000	9-12	43	0.54mm	0.73
2008.667	TC2002	5-8	40	0.61mm	0.69

**Table 1** – Summary of the Kfar-Hanassi network adjustment

#### 4. SECOND STEP: MOVEMENT ANALYSIS

The minimum constraints solution of the network benchmarks plane position for each monitoring epoch and their variance-covariance matrix are used as pseudo-measurements for the solution of the Second Step, where in each solution different models can be tested to describe the plane position of the network benchmarks.

For distance measurements the unknown scale factor can be different at different measuring epochs, especially when different instruments are used. Calibration of the distance meter right before or after to the measurement campaign can reduce the differences. This is important for in deformation analysis it is difficult to distinguish between the instrument scale factor and actual deformation.

##### 4.1 The Deformation Model

The position of a point  $x_i$  in time  $t$  is described in the linear model as equal to,

$$x_i = x_0 + \dot{x}\Delta t \quad (8)$$

where  $x_0$  is the plane location of the point at reference epoch  $t_0$ ,  $\dot{x}$  is the linear velocity of the point and  $\Delta t = t - t_0$ .

The observation equations for solving  $x_0$  and  $\dot{x}$  are rank deficient due to the lack of datum. There is a need to define a reference coordinate system for both  $x_0$  and  $\dot{x}$ , and thus the datum defect is double. The datum defect can be corrected by adding a corresponding number of constraints to the unknown parameters. Since the position axis of the network points is perpendicular to the time axis, there is no dependency between the datum definition of the coordinates of the network points ( $x_0$ ) and the velocity of the points ( $\dot{x}$ ). Consequently, changes in the datum definition, when defining  $x_0$ , do not affect the solution of  $\dot{x}$ . The constraints that apply to the network points could be different from those applied to the velocities. Hence, it is not necessary for the two reference systems to coincide. As we are interested mainly in the velocities, our concern remains with the selection and definition of a meaningful reference system for  $\dot{x}$ .

A unique solution of the datum problem can be achieved by adding a minimum number of constraints that equals the number of the datum defect (Koch, 1999). The defect of a 2D velocities network is two when the definition of origin is missing, and it can grow to four when the definition of the rotations and scale are missing as well. Geodetic measurements contain part of the datum definition. Therefore the exact size of the network defect is dependent on the type of the existing measurements. Distances can be assumed to have scale, therefore the size of the datum defect in a distance network is three, since the definition of origin and rotation is missing. For each monitoring campaign we may use the datum parameters that are contained in the distance measurements for estimating the coordinates of the network points, but not for estimating the velocities in the deformation analysis. Velocities are estimated based on a time series of monitoring campaigns. Therefore, when calculating velocities we should not reduce the datum defects to three due to the distances measurements but rather assume a datum defect of four parameters,  $d = 4$ .

## 4.2 The Statistical Tests

Statistical tests are applied for estimating the global congruency of the motion model and the significance of its parameters. Parameter  $\underline{x}$  that is derived from the measurements is tested, to

see if it is significantly different from parameter  $\underline{x}$  for a certain confidence level  $(1-\alpha)$ . The null hypothesis ( $H_0$ ) is tested against any alternative hypothesis ( $H_1$ ):

$$\begin{aligned} H_0 : \underline{x} &= x \\ H_1 : \underline{x} &\neq x \end{aligned} \quad (9)$$

When  $\underline{Q}_x$  is the cofactor matrix of  $\underline{x}$ , the null hypothesis is tested against the alternative hypothesis using the value  $w$  obtained from Equation (10) (Hamilton, 1964, Koch, 1999):

$$w = [(\underline{x} - x)^T \underline{Q}_x^{-1} (\underline{x} - x)] / h. \quad (10)$$

The calculated value  $w$  is tested against  $F(\alpha, h, r)$ , which is determined based on the Fisher distribution with the chosen significance level  $\alpha$ , the degrees of freedom  $r$ , and  $h$ , the rank of  $\underline{Q}_x$ . The null hypothesis is rejected if  $w > F(\alpha, h, r)$ .

### 4.3 Results

The free net solution, by using the Moore-Penrose inverse, of the linear motion model showed an a-posteriori variance factor of unit weight equaling  $\hat{m}_0^2 = 1.319$  (6), while the model's noise was  $\hat{w}^T P_x \hat{w} = 162.5$ . The redundancy of the first step provided 212 degrees of freedom (see Table 1) and the second step provided 72 degrees of freedom  $((12\text{points} \times 2) \times 5\text{campaigns} - (12\text{points} \times 2) \times 2)$  in total 284 degrees of freedom.

At the second step, the velocity ( $\dot{x}$ ) of the network points was tested. The null hypothesis  $H_0 : \dot{x} = 0$  was tested against the alternative hypothesis  $H_1 : \dot{x} \neq 0$ . As the dimension of velocities cofactor matrix  $\underline{Q}_{\dot{x}}$  equaled  $24 \times 24$  and its defect was 4, the rank of the matrix was  $h = 20$ . Thus  $F(5, 20, 284) = 1.61$  was obtained for an  $\alpha = 5\%$  level of significance. According to Equation (10)  $w = 9.62$ . Since  $w > F$  the null hypothesis was rejected at the significance level  $\alpha = 5\%$ , indicating that movements occurred during the campaigns.

A datum had to be defined in order to clarify which points moved. An S-transformation (Baarda, 1973) was applied to transform vector  $\dot{x}$  and its covariance matrix to a weight constrained solution. Congruency testing was performed to determine the stable datum points (as presented in Equation (10)) but the test statistic was applied only to the datum points.

In this paper four stable benchmarks (3, 4, 5 and 6) in the west bank of the Jordan River gorge were selected to define the datum (see Figure 1), because not all points in the east bank or in

the west bank can serve as datum. For a five percent level of significance,  $F(5, 4, 284) = 2.40$  was obtained. From Equation (10),  $w = 1.21$  was obtained. Because  $w < F$ , the null hypothesis was accepted, verifying that the four datum benchmarks were stable. The weight-constraint solution based on the datum definition is presented in Table 2.

<b>BM name</b>	$\dot{x}_{\text{east}}$ [mm/year]	$\sigma_{\dot{x}_{\text{east}}}$ [mm/year]	$\dot{x}_{\text{north}}$ [mm/year]	$\sigma_{\dot{x}_{\text{north}}}$ [mm/year]
0001	-0.22	0.05	-0.21	0.04
0002	-0.29	0.03	-0.23	0.04
0003	0.04	0.04	0.01	0.07
0004	0.00	0.03	0.00	0.04
0005	-0.06	0.04	-0.03	0.04
0006	0.03	0.05	0.02	0.09
0007	0.07	0.03	0.47	0.04
0008	0.09	0.04	0.34	0.04
0009	0.12	0.03	0.27	0.04
0010	-0.01	0.04	0.26	0.05
0011	0.16	0.04	0.55	0.06
0012	0.12	0.04	0.42	0.05

Table 2 - The weight-constraint solution of the linear model, where benchmarks 3, 4, 5 and 6 defined the network datum.

After setting a stable datum, a single point test was carried for all the other benchmarks in the network. If the null hypothesis was accepted for a single point then the point was considered stable at a significance level  $\alpha$ . Otherwise a significant movement was defined for the point. All benchmarks were found to have significantly moved (see Figure 2) relative to the reference benchmarks. The results of the single point tests are presented in Table 3.

<b>BM name</b>	<b>h</b>	<b>r</b>	<b>F(<math>\alpha, h, r</math>)</b>	<b>w</b>	<b>Significant</b>
0001	2	284	3.03	18.14	yes
0002	2	284	3.03	22.52	yes
0007	2	284	3.03	17.81	yes
0008	2	284	3.03	13.50	yes
0009	2	284	3.03	9.91	yes
0010	2	284	3.03	3.93	yes
0011	2	284	3.03	7.79	yes
0012	2	284	3.03	7.18	yes

Table 3 – Single point testing results for a significance level  $\alpha = 5\%$ .

Figure 2 depicts the behavior of the tested points for the linear model, when compared with the datum points. We can notice that the benchmarks located on the east bank (7, 8, 9, 10, 11

and 12) moved significantly mainly in the north direction relative to reference benchmarks. Benchmarks 1 and 2, which are located on the west bank approximately 500m west to the reference benchmarks moved significantly to the south-west direction.

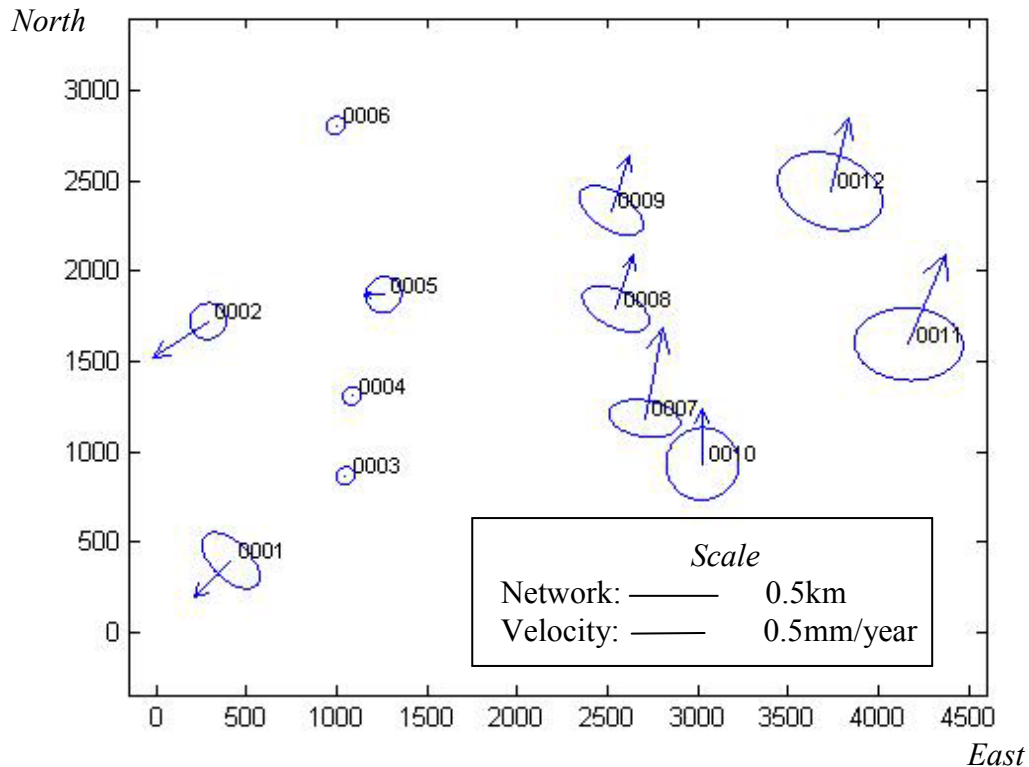


Figure 2 – The velocity field of the Kfar-Hanassi network relative to the datum points defined by benchmarks 3, 4, 5 and 6 . Analysis is based on five measuring campaigns carried out in 1990, 1991, 1992 1993 and 2008. Error ellipses depict the 95% confidence level.

## 5. DISCUSSION AND CONCLUSIONS

The goal of the Kfar-Hanassi network is to estimate the ongoing movement along the DSR. The relative movement between the two sides of the Dead Sea Rift could amount to a few millimeters per year. Based on GPS measurements the displacement between permanent sites which are located on both sides of the DSR is assessed to be less than 4 millimeters per year in the north-south direction (Wdowinsk et al., 2004). Using fault-locked model, the slip rate across the DSR is estimated at 3 to 4 millimeters per year (Wdowinsk et al., 2004).

A kinematic approach analysing the ongoing movement along the DSR based on the first four campaigns (between 1990 and 1993) was presented in Steinberg (1994). Analysis regarding

the displacement of a single point and movements of rigid blocks was presented in Vogel and Van Mierlo (1994). In both cases no significant movement along the DSR or deformation were detected.

The large time interval between the four campaigns measured between 1990 and 1993 and the one measured in 2008 dramatically increased the ability of the Kfar-Hanassi network to detect movements. Five distance measurement campaigns along a period of 18 years provide us with a very accurate description of current crustal movements in the Kfar-Hanassi region.

The mean velocity of the benchmarks located on the east bank of the Jordan River gorge relative to the datum points, located on the west bank of the river, is 0.38mm/year in the north direction and 0.09mm/year in the east direction. Benchmarks 1 and 2 which are located on the east bank (as the datum points) move at a rate of 0.22mm/year in the south-east direction. The results indicate a consistent trend of left-lateral motion along the DSR.

The detected significant movement between the banks of the Jordan River gorge and its slow rate may indicate that the DSR behaves as a locked fault. Additionally to the linear motion model, the locked fault model can be used to describe the plane position of the network benchmarks.

## **ACKNOWLEDGMENTS**

I am grateful to Yossi Melzer, head of the Research Department of the Survey of Israel and his team, which conducted professional distance measurements during the summer of 2008. I thank the Survey of Israel for providing me the Kfar-Hanassi campaigns data. I would like to thank Dr. Gershon Steinberg for his constructive and helpful remarks.

## **REFERENCES**

- Adler R and Pelzer H (1994). Development of a Long Term Geodetic Monitoring System of Recent Crustal Activity Along the Dead Sea Rift. Final scientific report for the German-Israel Foundation GIF.
- Baarda W (1973) S-Transformation and criterion Matrices. Netherlands Geodetic Commission, Publication on Geodesy, New Series, Vol. 5, No. 1.
- Chen, Y.Q., Kavouuras M., Chrzanowski A. (1987). A Strategy for Detection of Outlying Observations in Measurements of High Precision. *The Canadian Surveyor*. 41:529-540.

- Even-Tzur G. (2004). Variance Factor Estimation for Two-Step Analysis of Deformation Networks. *Journal of surveying engineering. Journal of Surveying Engineering*, 130(3):113-118.
- Ethrog U. (1991). Statistical Test of Significance for Testing Outlying Observations. *Survey Review*. 31:62-70.
- Hamilton W.C. (1964). *Statistics in Physical Science*. The Ronald Press Company, New-York.
- Karcz, I. (1994). Geological Considerations in Design of the Seminal Dead Sea Rift Network. *Perelmuter Workshop on Dynamic Deformation Models*, Haifa, Israel.
- Karcz, I., Forrai, J. and Steinberg, G., (1992). Geodetic Network for Study of Crustal Movements Across the Jordan-Deas Sea Rift. *Journal of Geodynamics*. 16:123-133.
- Koch, K.R. (1999). *Parameter Estimation and Hypothesis Testing in Linear Models*. Second Edition, Springer-Verlag, Berlin Heidelberg New-York.
- Papo HB, Perelmuter A (1993). Two-Step Analysis of Dynamical Networks. *Manuscripta Geodetica*. 18: 422-430.
- Van Mirlo J, Fahlbusch T., Oppen S (1990). Mekometer campaign and investigation in the Kfar-Hanassi network in 1990. Annual report of the year 1990 for the German-Israel Foundation GIF.
- Van Mirlo J and Fahlbusch T. (1991). Mekometer campaign and investigation in the Kfar-Hanassi network in 1991. Annual report of the year 1991 for the German-Israel Foundation GIF.
- Vogel M and Van Mierlo J (1994). Deformation Analysis of the Kfar-Hanassi Network. *Perelmuter Workshop on Dynamic Deformation Models*, Haifa, Israel.
- Wdowinski S, Bock Y, Bear G, Prawirodirdjo L, Bechor N, Naman S, Knafo R, Forrai Y and Melzer Y (2004). GPS measurements of current crustal movements along the Dead Sea fault. *Journal of Geophysical Research*. 109:1–16.

## CONTACTS

Gilad Even-Tzur  
Mapping and Geo-Information Engineering  
Faculty of Civil and Environmental Engineering  
Technion - Israel Institute of Technology  
Technion City, Haifa 32000  
ISRAEL  
Tel. +972-4-8293459  
Fax +972-4-8295708  
Email: [eventzur@technion.ac.il](mailto:eventzur@technion.ac.il)